

A CFD MODEL FOR THE IEA-R1 REACTOR HEAT EXCHANGER INLET NOZZLE FLOW

Delvonei A. Andrade, Gabriel Angelo, Gerson Fainer, Edvaldo Angelo, Pedro E. Umbehaun, Walmir M. Torres, Gaiânê Sabundjian, Luiz A. Macedo, Antonio Belchior Junior, Thadeu N. Conti, Bruno C. Watanabe and Caio C. Sakai

Instituto de Pesquisas Energéticas e Nucleares, IPEN - CNEN/SP
Av. Professor Lineu Prestes, 2242
05508-000 São Paulo, SP
delvonei@ipen.br , gabriel.angelos@gmail.com , gfainer@ipen.br

ABSTRACT

A previous preliminary model of the IEA-R1 heat exchanger inlet nozzle flow was developed and published in the International Nuclear Atlantic Conference-INAC-2009. A new model was created based on the preliminary one. It was improved concerning the actual heat exchanger tube bundle geometry. This became a very special issue. Difficulties with the size of the numerical mesh came out pointing to our computational system limits. New CFD calculations with this improved model were performed using ANSYS-CFX. In this paper, we present this model and discuss the results.

1. INTRODUCTION

This paper, developed by researchers of the Centro de Engenharia Nuclear (CEN) at IPEN – CNEN/SP, presents a study of the flow using computational fluid dynamics (CFD) for the inlet nozzle of IEA-R1 primary heat exchanger. It is based on a simplified preliminary model [1], published in the International Atlantic Conference – INAC-2009. ANSYS-CFX[®] [2] code is used as the CFD tool. The relevance of this study is the better understanding of the fluid dynamic, especially at the region of the shell holes given the complex geometry. Although the heat exchanger has been tested and approved for its operational conditions, it is not completely in accordance with TEMA [3] standard thermal design indications. Other authors [4,5] presented models to investigate the geometric characteristics of heat exchangers in order to optimize them.

IEA-R1 heat exchanger is of the type shell-and-tube, STHE [6], with one-pass shell and one-pass tube in countercurrent flow, Fig. 1. Its total length is 7 meters. It was commissioned in 2009 and its main operational characteristics are:

Mass flow rate, \dot{m} , is 188 kg/s and operational average pressure, p_{in} , is 5×10^5 Pa. Temperature difference, ΔT , is about 6.5 °C, [7]. IEA-R1 heat exchanger is projected to remove 5,015 kW which is the maximum power for the reactor primary circuit.

Figure 1a shows a general tridimensional view of the IEA-R1 shell-and-tube heat exchanger, STHE.

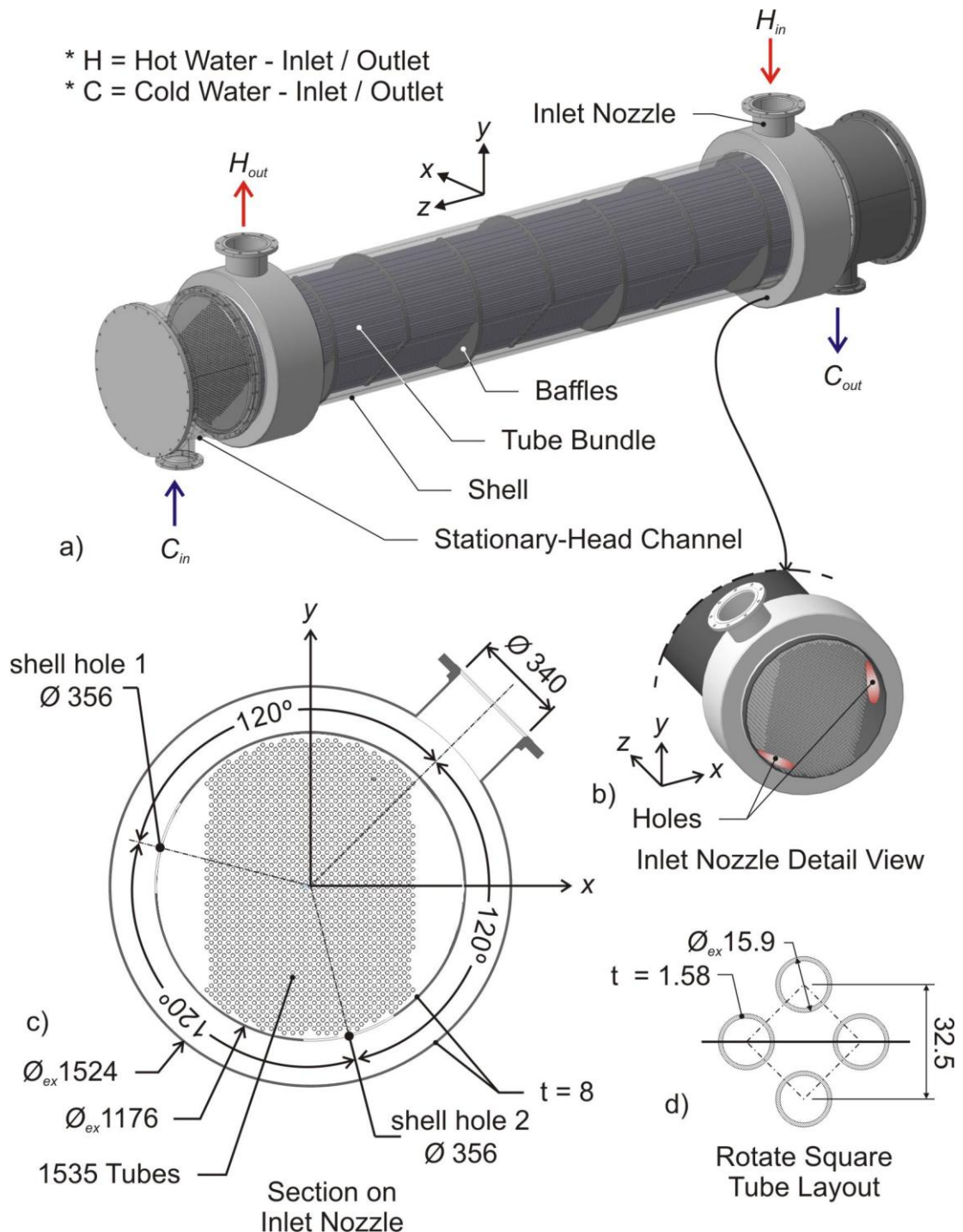


Figure 1. a) STHE general tridimensional view, b) Inlet nozzle detail view, c) Inlet Nozzle main geometry, position of the shell holes and main dimensions in millimeters, d) Tube bundle geometric characteristics in millimeters.

The geometry of the shell is transparent to allow the visualization of the internals: tube bundle, tubeplates and baffles. Inlet and outlet nozzles for the hot and cold fluid and stationary-head channel can also be observed. For the IEA-R1 STHE hot fluid is injected in the inlet nozzle into the shell passing through the baffles and tube bundle towards the outlet nozzle. Cold fluid removes the hot fluid heat and flows into the tube bundle in countercurrent flow as mentioned before.

A detailed tridimensional view of the inlet nozzle was drawn to show the shell holes, Fig. 1b, where an offset between the holes through the shell and the inlet nozzle can be observed.

The inlet nozzle geometry, position of the shell holes and main dimensions are shown by Fig. 1c.

Fig. 1d shows the tube bundle geometric characteristics, a rotate square layout [3,6].

2. NOZZLE MODEL

A tridimensional model was developed based on model presented in Fig. 1, using the finite volume method applied to a tetrahedral non structured mesh, Maliska, C. R. [8], Anderson, J. D. [9]. The equations considered are the mass conservation and momentum equation. Turbulence model considers $\kappa - \varepsilon$ model [10].

Operation fluid is water in stationary regime. Due to the small temperature variation in the inlet section, for this analysis flow is considered isothermal at 45 °C.

For the volumetric elements generation a degree of complexity shows up. It is related to the fact that some elements present aspect ratio of 100:1 as shown in Fig. 1c and Fig. 1d. It is illustrated when one compares the shell diameter to the small tube diameter in the tube bundle. So that the computational domain comes to a size as to test the computer system limits. A Xeon dual processor E5520 family, 2.26GHz, with 32 gigabytes of memory was used for the simulations which used approximately 88% of the available memory. This system has just been upgraded to 48 gigabytes of memory.

The tridimensional model geometry is shown in Fig. 2.

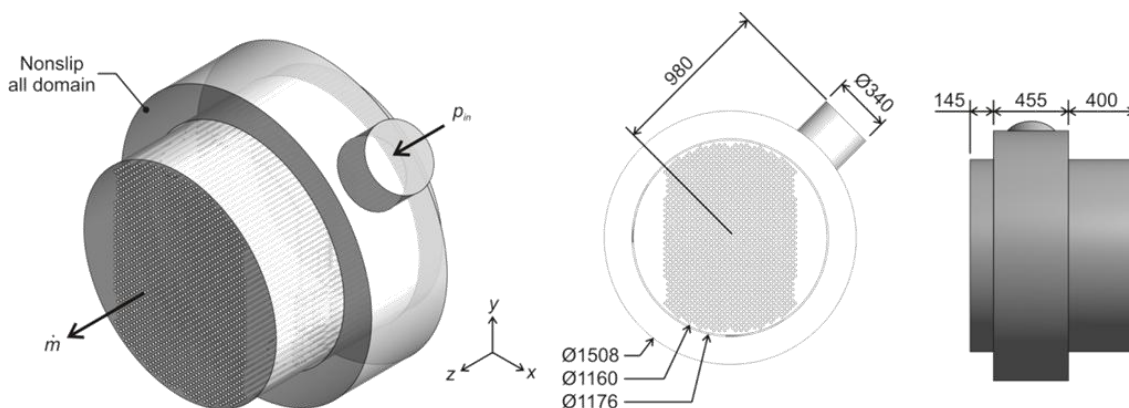


Figure 2. Tridimensional model, all dimensions in millimeters.

Fig. 3 presents the general mesh for this model. It was generated using the embedded delaunay algorithm for the superficial mesh. Advancing front mathematical algorithm was used for the volumetric elements, which is also within the code.

Mesh details are for section A – A can also be observed. A layer of tetrahedral elements was applied through the inflation option to some regions of the inlet nozzle. Inflation layer is good to resolve the near-wall physics giving support to achieve better results.

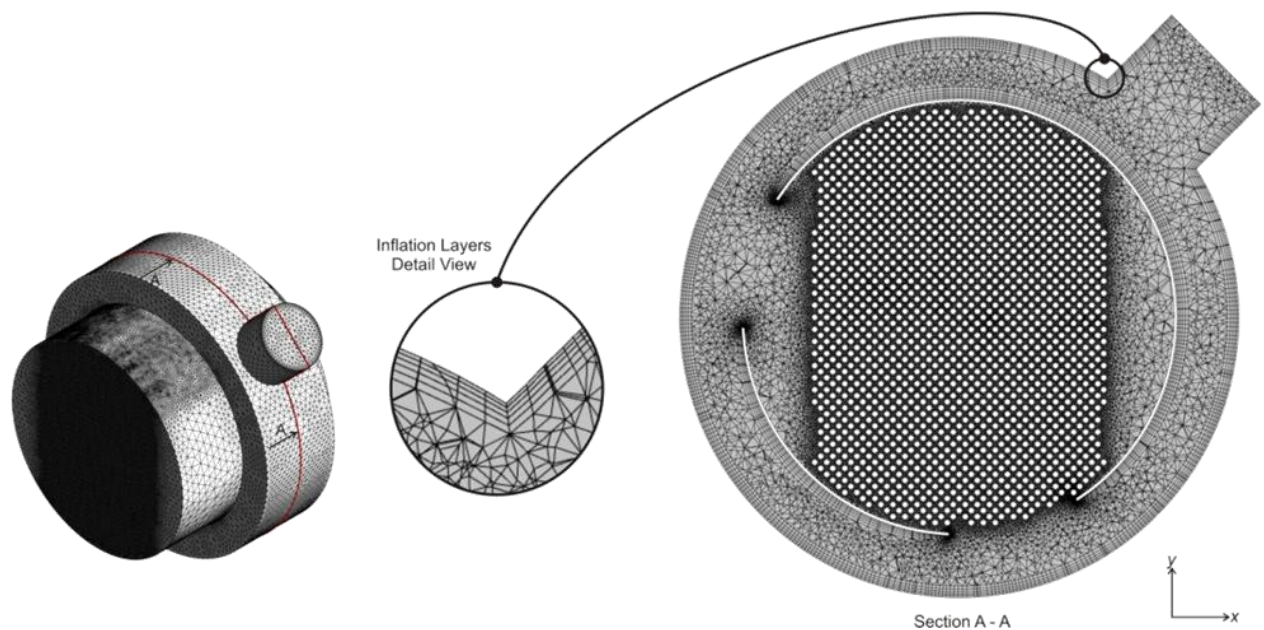


Figure 3. General model surface mesh, mesh detail view for section A – A and inflation layers detailed view.

For this model the computational domain has approximately 28 millions of volumetric elements.

In order to avoid turbulence behaviors as swirl, an increment of 400 mm was included in the outlet dimension of the heat exchanger.

Stern, F. at al. [11] and Wilson, R. V. at al. [12] present an approach to define and verify mesh. They discuss about mesh dependency on the results focusing the element size definition in order to validate the CFD models.

The methodology considers, for the same boundary condition, an increase of the mesh density using predefined ratios. This procedure must be performed in such a way that property variation or small variations are not present. When this condition is satisfied the solution is independent of the mesh.

This methodology was used in the present paper and the mesh presented in Fig. 3 is the last loop of this interaction. Intermediate meshes are not presented since results showed to be mesh dependent.

2.1. Boundary conditions

STHE parameters such as mass flux and operation pressure are known, however they are of difficult convergence to the proposed mathematical model.

At first it is assumed an average velocity for the inlet nozzle, v_e , 2.07 m/s based on the mass flux. Pressure at the outlet of the heat exchanger is equal to the operation pressure. Convergence criterion is controlled by setting the maximum residues to 0.0001 for all variables.

Results of this preliminary analysis were used to initiate the final resolution. In this case the operation pressure was set as the pressure at the inlet nozzle and mass flux was set as the boundary condition at the outlet. It guarantees variations of velocity at the inlet nozzle and variations of pressure at the heat exchanger outlet.

Non slip condition is applied to all other surfaces.

3. RESULTS AND DISCUSSION

Fig. 4 presents a contour for pressure for section AA showed by Fig. 3.

Pressure range in Fig. 4 considers the whole computational domain.

Fig. 4 shows that pressure is slightly bigger at the hole 2, nearer to the tube bundle, due to the smaller free passage area. The maximum pressure is near the inlet nozzle, where flow direction is changed abruptly.

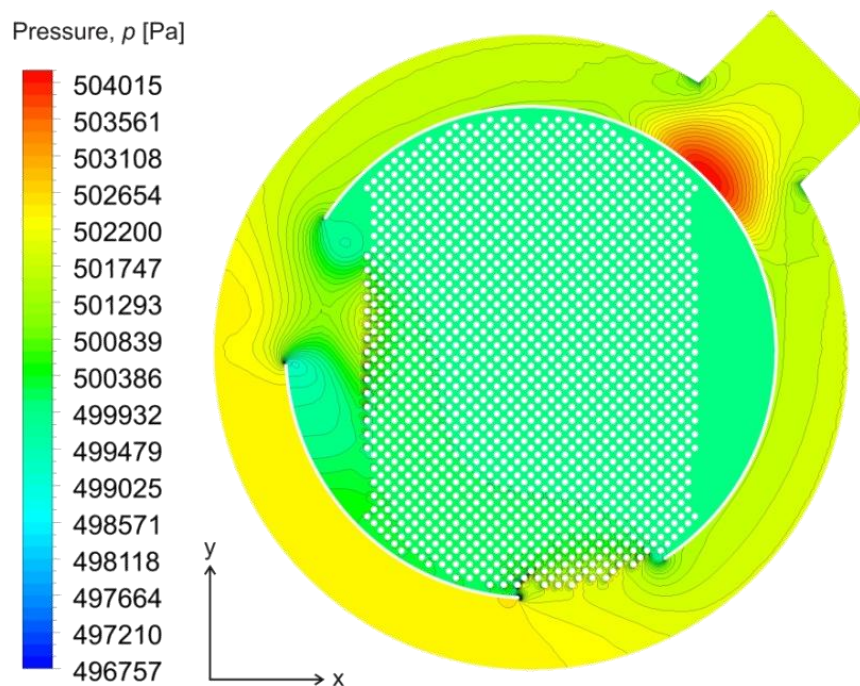


Figure 4. Pressure contour - section AA.

Velocity contour for section AA is shown by Fig. 5. Flow passing through hole 1 presents a higher velocity.

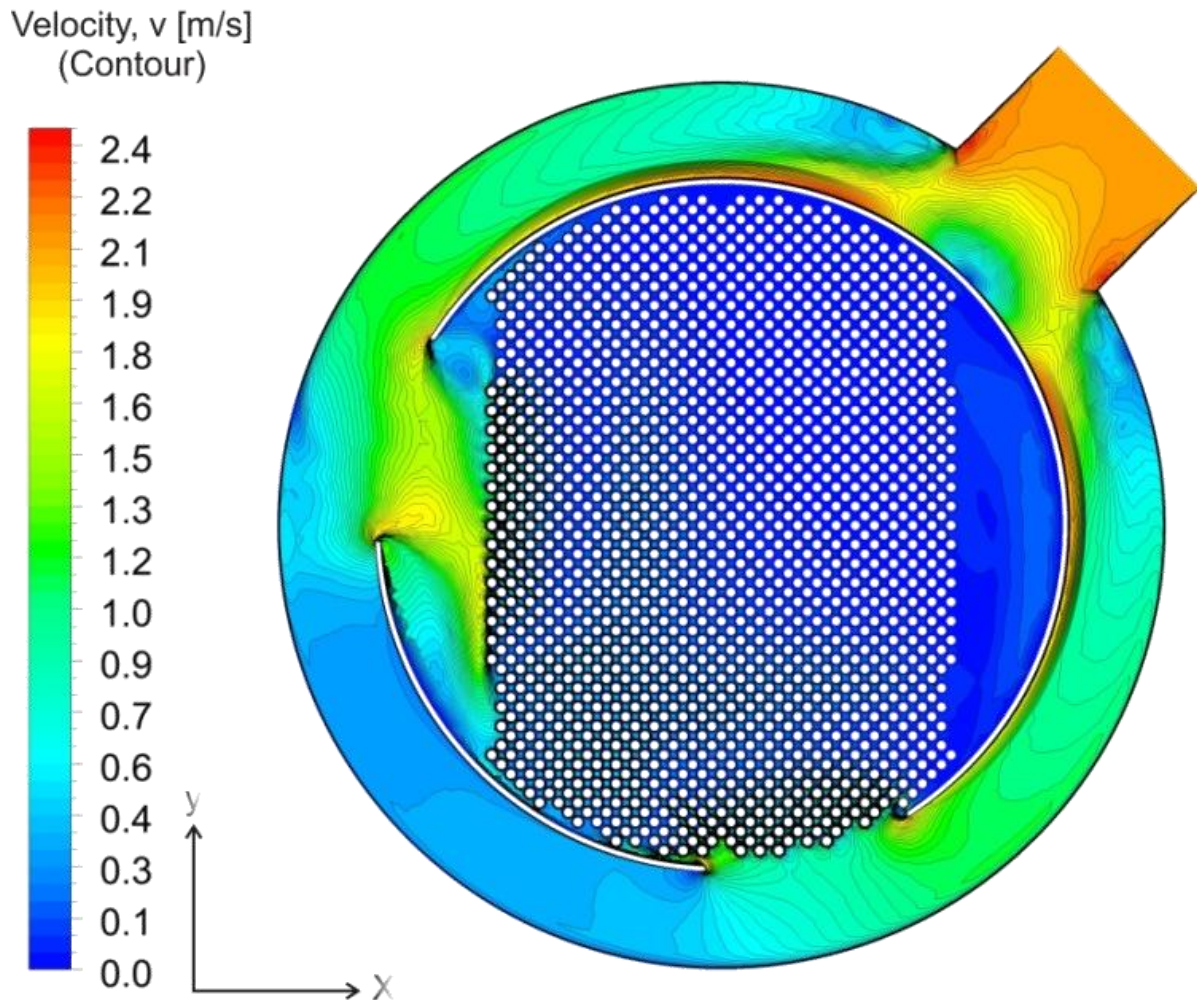


Figure 5. Velocity contour - section AA.

Streamlines for the velocity field are shown by Fig. 6a and Fig. 6b.

Vortex structures are observed. Flow at the regions of the holes is very complex due to tube bundle geometry constraint imposed to it. Streamlines near the holes 1 and 2, observed in Fig. 6a and Fig. 6b, illustrate the turbulent behavior.

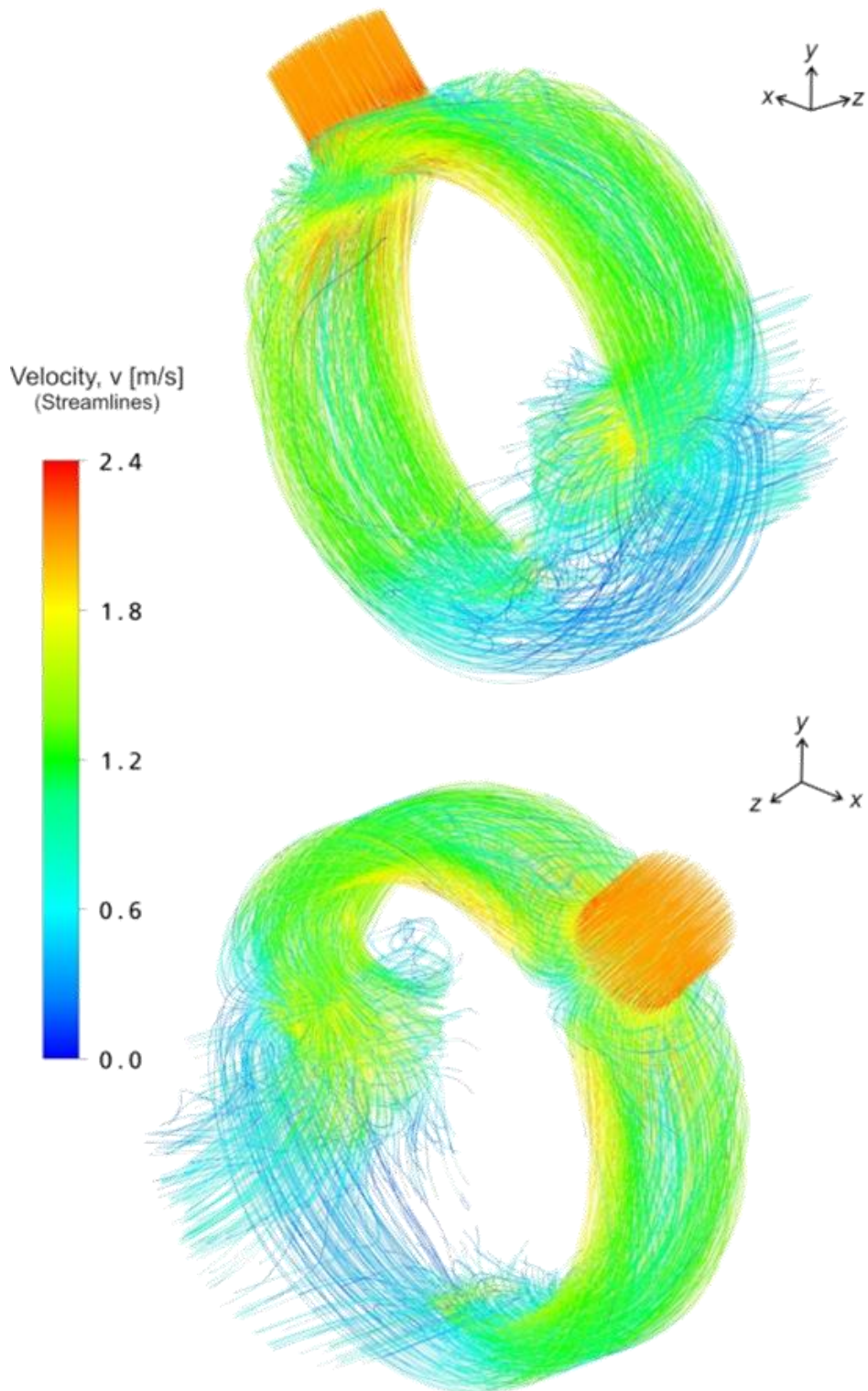


Figure 6. Velocity streamlines.

Fig. 7 presents velocity vector for section AA. Shell holes show different velocity field due to the different tube bundle distances as mentioned before. Swirl regions can be observed, especially near the regions of the shell holes.

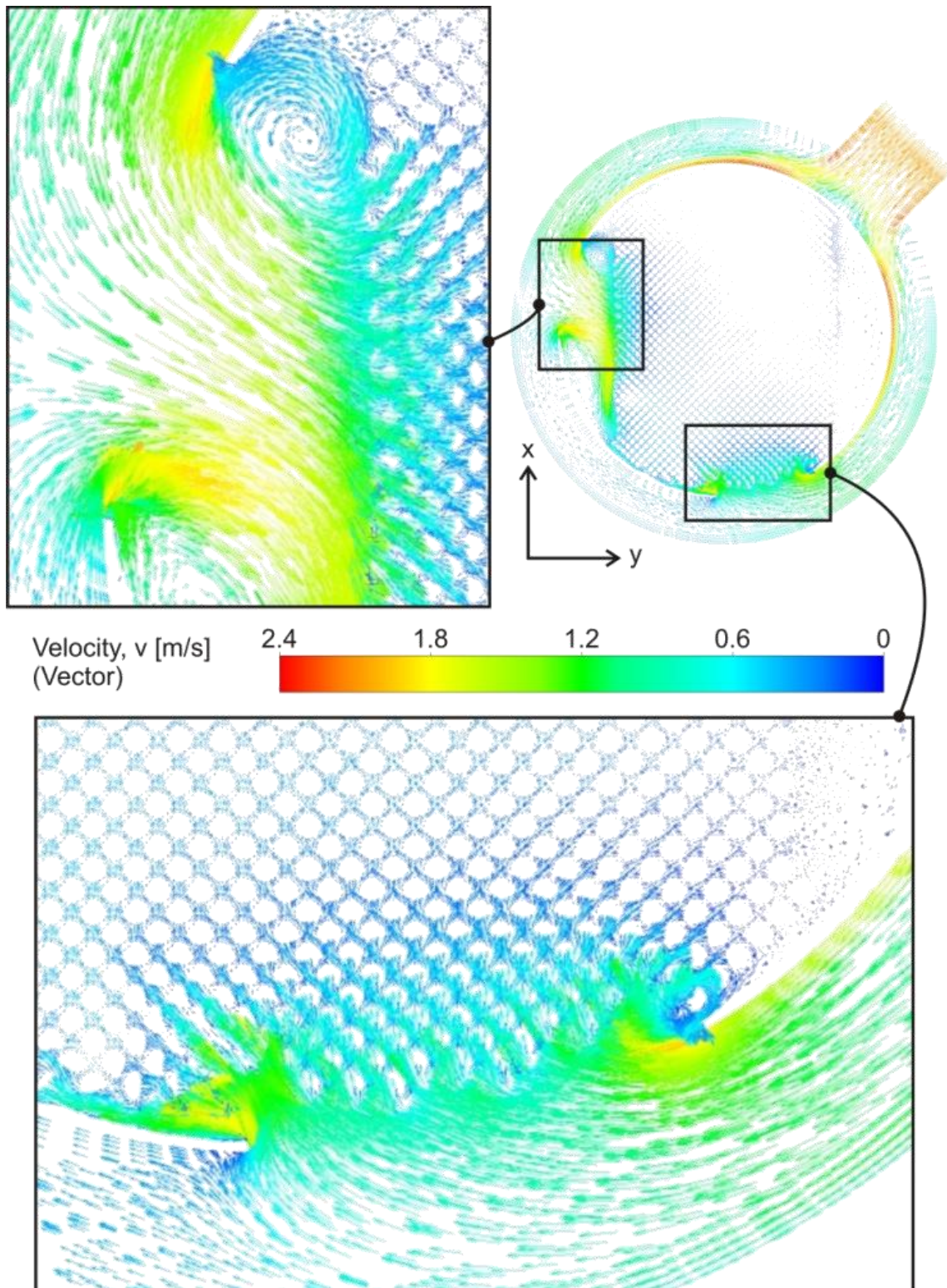


Figure 7. a) Velocity vector – shell hole 1, b) Velocity vector – Section A-A, c) Velocity vector – shell hole 2.

4. CONCLUSIONS

A study of the flow using computational fluid dynamics for the inlet nozzle of IEA-R1 primary heat exchanger was presented. The mathematical model results for the pressure field, velocity field, streamlines and vectors show consistency. This model led to satisfactory results. Mesh elements reached approximately 28 millions.

Many tests and simulations were performed to verify the mesh dependency and it worked to better understand the flow dynamics.

REFERENCES

1. Angelo, G. et al., Nuclear Research Reactor IEA-R1 Heat Exchanger Inlet Nozzle Flow – A Preliminary Study. *International Nuclear Atlantic Conference, INAC 2009*, Rio de Janeiro, RJ, Brasil, Sept. 27 - Oct. 2, (2009).
2. ANSYS-CFX – 11.0, *User Manual*, ANSYS Inc., Canonsburg, Pennsylvania – United States (2007).
3. Tubular Exchanger Manufacturers Association, *Standards of the Tubular Exchanger Manufacturers Association*, 8th ed., TEMA, Tarrytown, New York, USA (1999).
4. Wang, Q. et al., Numerical Investigation on combined multiple shell-pass shell-and-tube heat exchanger with continuous helical baffles, *International Journal of Heat and Mass Transfer*, Vol. 52, pp. 1214-1222 (2009).
5. Selbas, R. et al., A new design approach for shell-and-tube heat exchangers using genetic algorithms from economic point of view, *Chemical Engineering and Processing*, Vol. 45, pp. 268-275 (2006).
6. Mukherjee, R., Effectively Design Shell-and-Tube Heat Exchangers, *Chemical Engineering Progress* (1998).
7. Otomo, H., Especificação Técnica de montagem do Trocador de Calor do Sistema de Resfriamento do Reator IEA-R1, Relatório Técnico PSE.CENS.IEAR1.075.00 RELT.001.00, IPEN-CNEN/SP, São Paulo, SP, Brasil (2005).
8. Maliska, C. R., *Transferência de Calor e Mecânica dos Fluidos Computacional*, LTC – Livros Técnicos e Científicos Editora S. A., Rio de Janeiro, RJ – Brasil (2004).
9. Anderson, John D., *Computational Fluid Dynamics – The Basics with Applications*, McGraw-Hill, New York, NY – United States (1995).
10. Launder, B.E. and Spalding, D. B., The Numerical Computation of Turbulent Flows, *Computer Methods in Applied Mechanics and Engineering*, Vol. 3, pp. 269-289 (1974)
11. Stern, F. et al., Comprehensive Approach to Verification and Validation of CFD Simulations-Part 1: Methodology and Procedures, *Journal of Fluids Engineering*, Vol. 123, pp. 793-802 (2001).
12. Wilson, R. V. et al., Comprehensive Approach to Verification and Validation of CFD Simulations - Part 2: Application for Rans Simulation of a Cargo/Container Ship, *Journal of Fluids Engineering*, Vol. 123, pp. 803-809 (2001).